Astron. Astrophys. 306, 771–782 (1996)

ASTRONOMY AND ASTROPHYSICS

WR 22: the most massive Wolf-Rayet star ever weighed*

G. Rauw **[1], **J.-M. Vreux**[1], **E. Gosset** ***[1], **D. Hutsemékers**[1], **P. Magain** ***[1], **and K. Rochowicz**[2]

[1] Institut d'Astrophysique, Université de Liège, 5, Avenue de Cointe, B-4000 Liège, Belgium
[2] Institute of Astronomy, N. Copernicus University, ul. Chopina 12/18, PL-87100 Toruń, Poland

Received 19 April 1995 / Accepted 15 June 1995

Abstract. The results of an extensive spectroscopic campaign on the eclipsing binary WR 22 are presented. A new radial velocity curve is deduced for the WN7 component, allowing us to improve the parameters of the orbit, formerly determined on the basis of photographic spectra. The high signal-to-noise ratio of our data also allows the detection of some weak absorption lines which, for the first time, can definitely be attributed to the companion. A study of their radial velocities gives a mass ratio of $m_{\rm WR}/m_{\rm O} = 2.78$ leading to a minimum mass of 72 $M_\odot$ for the WN7 star. The companion can be classified as a "late O" (O6.5-O8.5) star with a luminosity ratio of the system $q = L^y_{\rm WR}/L^y_{\rm O}$ at 5500 Å of about 8. The exceptionally high mass of the WN7 star and its high hydrogen mass-fraction suggest that WR 22 is at the beginning of its Wolf-Rayet evolution. As a matter of fact, with such a high mass, WR 22 most probably is still a hydrogen burning object. Therefore, the WN7 component is much closer to a main sequence O star with a "Wolf-Rayet clothing" than to the other members of the Wolf-Rayet family, which are rather highly evolved He-burning descendants of massive progenitors.

Key words: stars: individual: WR 22 – stars: Wolf-Rayet – binaries: spectroscopic – binaries: eclipsing – stars: fundamental parameters

1. Introduction

Wolf-Rayet (hereafter WR) stars are hot, luminous objects representative of the late stage of evolution of massive O stars. Their characteristic emission-line spectrum is produced in a dense and energetic stellar wind that peels off the outer layers of the star. Intrinsic absorption lines are generally absent from their spectra. The atmospheres of WR stars of the nitrogen sequence (WN) exhibit CNO processed material, while hydrogen is strongly depleted or completely absent (Maeder & Conti 1994).

Among these objects, the WN7+abs stars form a special group. They have particularly high velocity winds and high luminosities, a considerable hydrogen content and their spectra exhibit absorption components in the upper Balmer series (Crowther et al. 1995a). Since some of the late WN stars (WNL) share many properties with the Of stars, Conti (1976) suggested that they could form an evolutionary link between the most massive single Of stars and the other WR subtypes.

Observationally, most Population I WR stars appear to originate from O stars with initial masses higher than 40 $M_\odot$ (e.g. Conti et al. 1983). However, the exact evolutionary sequence of single massive O stars is still unknown (e.g. Langer et al. 1994, Meynet et al. 1994, Crowther et al. 1995b). In addition, there is a division of opinion on the importance of mass transfer in the evolution of O + O binary systems (De Greve 1991, Maeder & Meynet 1994). Crowther et al. (1995b) suggest that single WNL+abs stars descend from very massive progenitors ($m_{\rm initial} \geqq 60 M_\odot$) without a previous excursion into the Luminous Blue Variable (LBV) or red supergiant (RSG) phase and evolve through the sequence: O → Of → WNL+abs → WN7 (→ WNE) → WC → SN, whereas the less massive stars are believed to evolve through an RSG or LBV phase before they enter the WN8 stage. Since all these evolutionary models strongly depend on the initial mass of the progenitor, an accurate observational determination of WR masses is essential.

In this context, WR 22 (≡ HD 92 740), a bright ($V \sim 6.4$) WR binary of spectral type WN7+abs, is certainly one of the most suited systems to provide a first reliable determination of the mass of a WN7+abs star. WR 22, a member of the Carina OB1 association (Lundström & Stenholm 1984), is classified as a single-lined spectroscopic binary (SB1) (van der Hucht et al. 1981, 1988). The spectrum of the WR star exhibits a considerable amount of hydrogen ($X_{\rm H} \sim 40\%$, Hamann et al. 1991, Crowther et al. 1995a). In addition to the typical strong WR emission lines, the spectrum displays absorption lines of the upper Balmer series whose wavelengths vary in phase with the emission lines. These absorption lines thus belong to the WR component (Niemela 1973, Moffat & Seggewiss 1978 hereafter

Send offprint requests to: G. Rauw

* Based on observations collected at the European Southern Observatory, La Silla, Chile.

** Aspirant au Fonds National de la Recherche Scientifique (Belgium)

*** Chercheur Qualifié au Fonds National de la Recherche Scientifique (Belgium)

Table 1. Heliocentric radial velocities of WR 22 (in km s^{-1}), as measured on our spectra. Mean values from two or more spectra are marked by asterisks

JD	Instrument	Exposure		ϕ	v_{rad}(WN7 star)		v_{rad}(O star)		
(2440000+)	(ESO)	(s)			N IV λ4058	H9	H9	He I λ4026	He I λ4471
6575.480	2.2 m+B&C	480		0.780	–78.7				
6576.506	2.2 m+B&C	390		0.793	–83.6				
6577.493	2.2 m+B&C	600	*	0.805	–85.2				
6578.474	2.2 m+B&C	2520	*	0.818	–81.3				
6888.658	CAT+CES	7200	*	0.679					76.36
6892.670	2.2 m+B&C	540	*	0.729	–78.1				
6893.565	CAT+CES	1800		0.740		–125.22			
6893.603	2.2 m+B&C	600	*	0.741	–80.1				
6894.616	2.2 m+B&C	540	*	0.753	–71.6				
6895.624	2.2 m+B&C	300		0.766	–84.0				
6896.672	2.2 m+B&C	600	*	0.779	–65.4				
6897.616	2.2 m+B&C	540		0.791	–79.7				
7233.091	CAT+CES	4200	*	0.967		–179.92			
7233.895	CAT+CES	3000		0.977		–176.30			
7233.991	CAT+CES	900	*	0.978	–70.74				
7234.011	CAT+CES	3600	*	0.979	–69.01				
7235.820	CAT+CES	1800	*	0.001					94.9
7236.553	CAT+CES	1800		0.010		–124.13			
7238.614	CAT+CES	1800		0.036		–74.64	–126.8		
7238.802	CAT+CES	1800		0.038					–106.3
7619.529	CAT+CES	3600	*	0.778		–126.99	156.6		
7630.506	1.5 m+B&C	1200	*	0.915					215.1
7665.500	CAT+CES	3600	*	0.350		–78.95	–61.9		
7683.514	CAT+CES	3600	*	0.575		–91.64			
7698.495	CAT+CES	3600	*	0.761		–132.25	133.3		
7857.842	CAT+CES	4200	*	0.745		–135.15			
7877.816	CAT+CES	7200	*	0.994		–114.38			
7878.789	CAT+CES	5400	*	0.006		–111.06			
7952.646	CAT+CES	5400	*	0.925		–174.05			
7952.781	CAT+CES	1200	*	0.927	–99.78				
7953.569	CAT+CES	1200	*	0.937	–95.60				
7953.644	CAT+CES	2700	*	0.938				195.3	
7953.697	CAT+CES	4200	*	0.938					208.1
7954.585	CAT+CES	5400	*	0.949		–164.19	240.6		
7954.758	CAT+CES	1800		0.952	–87.24				
7955.580	CAT+CES	5400		0.962		–156.67			
7955.788	CAT+CES	1800		0.964	–79.52				
7955.871	CAT+CES	3600		0.965				150.7	
7956.584	CAT+CES	5400		0.974		–157.67			
7956.806	CAT+CES	1800		0.977	–67.55				
7956.878	CAT+CES	3600		0.978				133.3	
7957.583	CAT+CES	5400		0.987		–121.23	123.8		
7957.805	CAT+CES	1800		0.989	–39.67				
7957.878	CAT+CES	3600		0.990				79.1	
8049.512	CAT+CES	7200	*	0.131		–61.00			
8055.482	CAT+CES	3600	*	0.206	23.12				
8055.587	CAT+CES	5400	*	0.207		–76.47			
8390.515	CAT+CES	5400	*	0.377	–8.03				
8392.548	CAT+CES	7200	*	0.402		–81.48			
8400.477	CAT+CES	3600	*	0.501	–27.32				
8400.519	CAT+CES	2700		0.501				40.8	
8681.608	CAT+CES	3600	*	0.000	–29.47				
8681.721	CAT+CES	3600		0.002				–64.0	
8681.790	CAT+CES	3600		0.003		–88.32			

Table 1. (continued)

JD	Instrument	Exposure		ϕ	v_{rad}(WN7 star)		v_{rad}(O star)	
(2440000+)	(ESO)	(s)			N IV λ4058	H9	He I λ4026	He I λ4471
8682.583	CAT+CES	3000		0.013	4.42			
8682.714	CAT+CES	3600		0.014			–67.3	
8682.793	CAT+CES	5400	*	0.015		–71.33		
8683.582	CAT+CES	3600		0.025	21.93			
8683.735	CAT+CES	3600		0.027			–95.9	
8683.806	CAT+CES	5400	*	0.028		–58.46		
8688.564	CAT+CES	3000		0.087	39.93			
8688.689	CAT+CES	3600		0.089			–198.5	
8688.804	CAT+CES	1800		0.090				–167.6
8689.559	CAT+CES	3000		0.099	31.46			
8689.693	CAT+CES	3600		0.101			–212.8	
8689.807	CAT+CES	5400	*	0.102		–43.87		
8689.884	CAT+CES	3000	*	0.103				–184.3
8690.558	CAT+CES	3000		0.112	40.98			
8690.676	CAT+CES	3600		0.113			–203.2	
8691.556	CAT+CES	3000	*	0.124	37.38			
8691.766	CAT+CES	6000	*	0.127		–73.01		
9471.074	1.5 m+B&C	2400	*	0.834	–90.1		166.9	158.8

M&S, Conti et al. 1979 hereafter CNW). Previous studies led to a rather eccentric ($e \sim 0.55$), 80.35 day orbit (M&S 1978, CNW 1979). The only potential detection of the companion was reported by Niemela (1979) and CNW, who found very weak auxiliary absorptions on a few of their spectrograms. Since 1989, WR 22 is known to be an eclipsing binary (Balona et al. 1989, Gosset et al. 1991), with only one eclipse (corresponding to the WR in front of its companion) being visible. This discovery implies that the companion must be a luminous object and should therefore exhibit at least a weak spectral signature.

In the present paper, an extensive amount of spectroscopic data collected over several years is used to improve our knowledge of WR 22. The observations collected during this campaign are presented in Sect. 2; in Sect. 3, the data are used to set up a new orbital solution for the WN7 primary. A careful investigation of the spectra also allows to detect absorption lines belonging to the secondary. These features are used in Sect. 4 to investigate the mass ratio of the system and to attempt a spectral classification of the companion. Finally, in Sect. 5 the results are briefly discussed in the context of modern evolutionary scenarios.

2. Observations and data reduction

2.1. High resolution spectra

In order to detect a weak spectral signature of a faint companion and to achieve a high precision on radial velocity (RV) measurements, high signal-to-noise spectra with relatively high dispersion are required. Therefore, after investigations at lower resolution (see below) and forced to recognize that such a program would only be accepted with difficulty on a bigger telescope, a long spectroscopic campaign was initiated using the Coudé Echelle Spectrometer (CES) fed by the 1.4 m Coudé Auxiliary Telescope (CAT) at the European Southern Observatory (ESO, La Silla). Several observing runs were conducted, mainly around phases $\phi \sim 0.9$ and 0.1, to cover the nodes of the orbit and therefore to achieve the highest possible shift in radial velocity between the WN7 star and its companion. Given the rather long period of WR 22 (80.3 days), it took about eight years to collect sufficient data.

More than 200 CES spectra were obtained between 1987 and 1992. The CES was used in the Short Camera mode. The detector was ESO CCD#9 (Schwarz & Melnick 1993), an RCA 1024 × 640 pixel CCD with a readout noise of about 33 e^- and a pixel size of 15 × 15 μm^2. The resolving power lies between 50 000 and 60 000. The mean S/N ratio, evaluated at continuum level, is about 230. Many different wavelength settings between 3700 and 4700 Å were covered and comparison exposures of a Thorium-Argon hollow cathod lamp were secured for each of them.

All the observations were reduced using the MIDAS software. The spectra and flat field exposures were corrected for the non-linearity effects of CCD#9 reported by Gosset & Magain (1993).

One of the most critical steps in analyzing WR spectra with broad emission lines is the normalization to the continuum. In the present case, the problem is even worse due to the very limited spectral range available (typically about 35 Å) and the sometimes very peculiar shape of the response curve. We therefore decided to use the lower resolution spectra as a template to reduce the CES data.

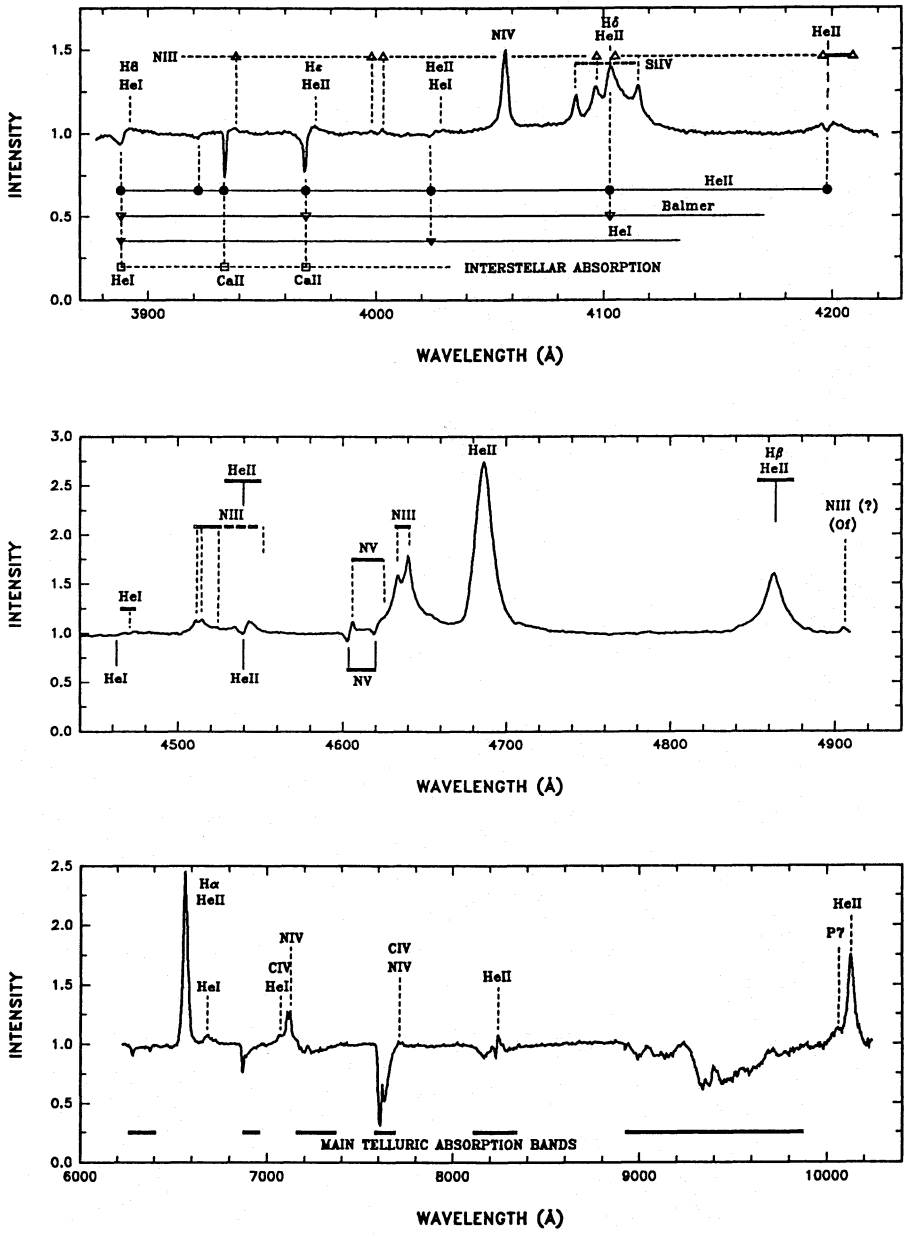

Fig. 1a–c. The spectrum of WR 22 in the wavelength ranges 3880 - 4220Å (**a**), 4450 - 4910Å (**b**) and 6200 - 10200Å (**c**), as normalized to the continuum. The main lines are identified, above the spectrum for the emissions and below for the absorptions. Interstellar lines and telluric bands are also indicated. See text for dates and more details

2.2. Low resolution spectra

A set of low resolution spectra in the blue region was obtained in 1986 and 1987 at the ESO/MPI 2.2 m telescope equipped with a Boller & Chivens (B&C) Cassegrain Spectrograph, giving a spectral coverage from 3860 to 4220 Å with a reciprocal dispersion of 29 Å/mm. The detector was a GEC 576×385 CCD with pixel size 22 × 22 μm^2. The slit width used was 171 μm corresponding to 2″ on the sky. Comparison exposures of He-Ar lamps were made each time the telescope was pointed at another target. The mean S/N ratio is about 160. As an illustration the spectrum of April 8, 1987 is displayed in Fig. 1a along with the identifications of the most important lines.

Several spectra of WR 22 covering the wavelength-range 4427–4915 Å were also acquired in March 1989 at the ESO 1.5 m telescope linked to the B&C spectrograph. The slit was set to 2″.2 . The grating (1200 lines/mm, ESO grating #11) was used in the second order, providing a reciprocal dispersion of 29 Å/mm, while the first order was blocked out via an RG850-BG38 filter. The detector was an RCA 1024 × 640 CCD (ESO CCD #13, Schwarz & Melnick 1993). The mean spectrum of the first night (March 7/8) is shown in Fig. 1b.

A few additional spectra were collected in 1994 with the same equipment as for the 1989 mission, but with a holographic grating (2400 lines/mm, ESO grating #32) providing a reciprocal dispersion of 32.6 Å/mm over the range 3875 to 4875 Å. The detector used was a Ford Aerospace 2048L UV-coated CCD (ESO CCD#24, Schwarz & Melnick 1993) with a pixel size of 15 × 15 μm^2. The conversion factor was 2.9 e^-/ADU.

Finally, a red spectrum was taken during an earlier mission in February 1982 with the ESO Reticon system (Dennefeld et al. 1979) attached to the B&C spectrograph at the ESO 1.5 m

telescope (Vreux et al. 1983). The slit used was 150 μm wide, corresponding to 3″ on the sky. The domain covered was 5700–10890 Å. The normalized spectrum is displayed in Fig. 1c.

All the reductions were performed using either the IHAP or the MIDAS software.

3. The orbit of the WN7 component

Until now, the orbital parameters of WR 22 were determined on the basis of photographic spectra only (M&S 1978, Niemela 1979, CNW 1979). From these former studies, it became obvious that the orbital motion of the WN7 component was best derived from the RV's measured on the narrow N IV λ4058 emission line. Indeed this line has been shown to form in the deeper layers of the WR stellar wind, thus reflecting the actual motion of the star much better than lines formed farther out in the wind (CNW 1979). Table 1 gives the journal of RV measurements for several lines.

The central wavelength of the N IV λ4058 line was determined by fitting a Gaussian profile above three different intensity levels over the continuum: $\sim 0.05\,I_{\rm max}$, $0.50\,I_{\rm max}$ and $0.80\,I_{\rm max}$, where $I_{\rm max}$ is the normalized intensity of the emission-line peak. The mean of the three values was then used to compute the radial velocity, whereas the standard deviation around this mean value enabled us to estimate the error on the velocity due to the asymmetry of the line. This error turned out to be very small, about $2.7\,10^{-2}$Å i.e. 2 km s^{-1}, for the N IV emission, whereas for the Balmer absorption lines H8, H9 and H10, a similar method indicates much higher errors, due to phase dependent profile variability and blending effects.

On the other hand, there exists also an error due to the limited spectral resolution and the accuracy of the wavelength calibration, which can be evaluated using the standard deviations of the measured RV's of some prominent interstellar lines such as He I λ3889 and Ca II λ3934: results are given in Table 2 below. The values of this table show that the accuracy of the B&C data is mainly limited by resolution, whereas the CES data are limited by profile asymmetry. One should notice that our RV's for the interstellar matter are in good agreement with the values given by Walborn & Hesser (1975) who derived +5.4 km s^{-1} for Ca II and –27 km s^{-1} for He I from their 9 Å mm^{-1} coudé spectra of several stars in the direct neighbourhood of WR 22. The equivalent widths measured on our CES spectra amount to 0.349 ± 0.002 Å and 0.015 ± 0.001 Å for Ca II λ3934 and He I λ3889 respectively.

Applying the method of Lafler & Kinman (1965) to the RV's they derived, M&S (1978) as well as CNW (1979) found an orbital period of 80.35 days. As these RV's were measured on photographic plates, the expected uncertainties are rather large. Since WR 22 was shown to be an eclipsing binary (Balona et al. 1989, Gosset et al. 1991), several eclipses have been observed by our group, allowing us to check the period deduced from RV analyses by folding the photometric data in a phase diagram. In this way, we found a somewhat lower value of 80.310 ± 0.010 days (Rauw et al. 1995). However, recent photometric data show that the best compromise between eclipses and RV's is obtained for 80.325 ± 0.010 days. The uncertainty of ~0.010 day indicates the range of periods for which an acceptable compromise is achieved between the requirement of low scatter around the radial velocity curve and the constraint of overlapping the different eclipses.

Table 2. Mean values and standard deviations of the measured RV's (in km s^{-1}) of two interstellar lines in the spectrum of WR 22

Line	Instrument	Mean RV	σ	Number of spectra
He I λ3889	CAT+CES	–24.8	0.9	26
Ca II λ3934	CAT+CES	+6.4	0.8	7
Ca II λ3934	2.2 m+B&C	+4.5	6.4	15
Ca II λ3934	1.5 m+B&C	+5.9	2.1	4

A least square radial velocity curve was derived using the program of Wolfe, Horak & Storer (1967). The resulting orbital parameters are given in Table 3. Comparing our N IV orbital solution to the former studies, we notice that the elements of M&S (1978) agree within their uncertainties with our results, while the best solution of CNW (their Group 1 parameters) yields a somewhat higher eccentricity e (0.64) and also a higher velocity semiamplitude K (77 km s^{-1}).

Due to the high resolution of the CES spectra, the observed RV's of N IV λ4058 show a rather low scatter around the computed solution (Fig. 2). Besides the lower dispersion data around ϕ=0.75–0.80, the most important deviations occur after periastron, near the ascending node of the orbit. Given the high eccentricity, this scatter could result from tidal deformations of the emitting area in the WR stellar wind after periastron passage.

The argument of periastron $\omega = 271\overset{\circ}{.}6$ shows that the eclipse and periastron nearly coincide (Rauw et al. 1995). The resulting time of periastron passage (T_0) is in excellent agreement with the date of the eclipse observed around JD 2 449 323.8 (December 2, 1993).

RV's were also measured for the H9 Balmer absorption line of the WN7+abs star. Computing an independent radial velocity curve for these absorptions leads to important differences in the orbital parameters (a higher eccentricity, a lower K,...). Similar results were already obtained by CNW (1979) and M&S (1978). On the other hand, when setting all the orbital parameters of the absorption line radial velocity curve (except the systemic velocity γ) to the values derived from the N IV solution, a good agreement is achieved for $\gamma \sim -110$ km s^{-1} for the H9 line, i.e. by shifting the N IV solution by –80 km s^{-1}. The corresponding curve is shown in Fig. 2.

Although there is some scatter around this curve, we believe this second approach to be the most realistic one. First, as a result of the difficulties in defining the center of the absorption features, the uncertainties on our measurements are much higher for H9 than in the case of the N IV emission line. Second, some differences between the observations and the predicted curve can be explained qualitatively by the blending of the WR line by the absorption line of a less massive companion (see Sect.

Table 3. Orbital parameters from the RV's of WR 22 (P=80.325 days). The quoted uncertainties are probable errors

	WR star			O star*		
	N IV λ4058			He I λλ4026,4471 & H9		
e	0.559	±	0.009			
γ (km s^{-1})	−29.8	±	0.7	21.3	±	7.0
K (km s^{-1})	72.3	±	1.0	201.4	±	10.0
ω (°)	271.6	±	1.9			
T_0 (JD 2 440 000 +)	9324.17	±	0.2			
$a \sin i$ (km)	6.63 10^7	±	0.1 10^7	1.85 10^8	±	0.1 10^8
$f(m)$ ($M_\odot$)	1.795			38.800		
$m \sin^3 i$ ($M_\odot$)	71.7			25.7		
mean$\|O-C\|$ (km s^{-1})	4.3			24.0		

* Orbital solution computed adopting e, ω, T_0 from the N IV WR solution.

4.1). This is particularly clear at phases between $\phi \sim 0.1$ and 0.25, where the observed RV's are lower than expected, and at phases between $\phi \sim 0.3$ and 0.75, where they are higher than expected. Finally, some line-profile variability takes place in some of the emission lines or P-Cygni emissions and could affect the RV's of the absorption components. However, discussing these variations is beyond the scope of the present paper and additional data are still collected in order to investigate these variations.

Similar conclusions can be drawn for the RV's of the H8 and H10 absorptions. In order to explain the blueshifted systemic velocity of the Balmer absorption lines, CNW referred to the outwards velocity gradient in the envelope of the star. However, model calculations kindly performed at our request by Hamann (1995) suggest that the RV's of the Balmer absorptions should be interpreted as a result of the blend of these lines with the absorption components of the He II Pickering series.

4. The spectral signature of the companion

Until now, the only potential detection of a spectral signature of the secondary star in WR 22 has been reported by Niemela (1979) and CNW (1979), who found some very faint absorptions on a few of their spectrograms, taken when the expected Doppler shift between the lines of the WR and those of the companion was the highest.

A careful investigation of our high resolution spectra allowed us to detect some features moving 180° out of phase with the lines of the WN7. The first lines we identified were He I λλ4026, 4471 and H9. A close look at the 1994 low resolution spectra revealed that both He I absorptions were also visible on these spectra. Since the absorptions we are measuring are very weak, their position can only be measured by visual estimation of the central wavelength. Thus the RV's are plagued with uncertainties of about 20 km s^{-1}. However, the RV's derived from these three lines are in good agreement with each other. In order to check that these features are consistent with the spectral signature of the companion, we searched for other lines with similar RV's. The results, listed in Table 4, include some He II lines, thus identifying the secondary as an O star.

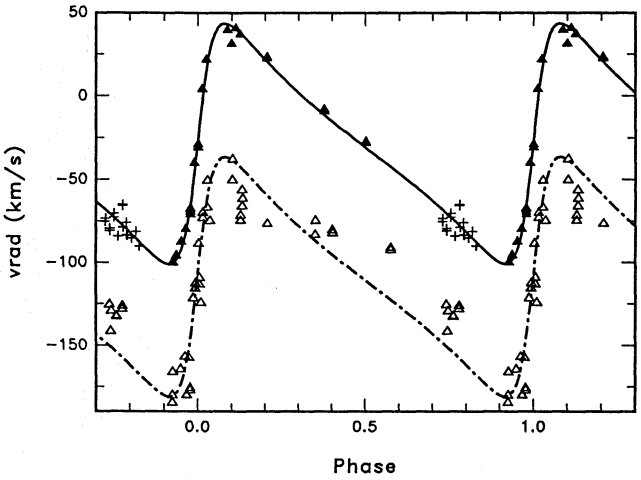

Fig. 2. Radial velocities of the N IV λ4058 emission line and of the H9 absorption line in a P=80.325 days phase diagram. Filled and open triangles are for CAT+CES spectra of, respectively, N IV λ4058 and H9. Crosses (+) are for lower resolution B&C spectra of N IV λ4058. The solid line shows the least square orbital solution for the emission line, whereas the dashed-dotted line shows the same solution with γ shifted by −80 km s^{-1}, corresponding to the adopted best solution for H9

Although we have a good phase coverage for some of the interesting wavelength ranges, the companion was not detected on all our spectra. There are several reasons for this:

- the eclipse of the secondary by the WN7 primary: none of the companion lines could be measured at phases close to periastron;
- the phase dependent blending with the WR lines: owing to the γ velocity of some of the WR lines (e.g. the Balmer absorptions), blending occurs over a rather wide phase domain not necessarily centered on periastron (see the forthcoming Fig. 6 and Sect. 4.1);
- the phase dependent blending with interstellar absorptions, e.g. interstellar He I λ3889 affecting H8 (see Fig. 4 below).

Table 4. Absorption lines of the secondary of WR 22

Line	mean(W_λ) (Å)	σ (Å)	Number of measurements	Comments
H10	0.076	0.008	5	
H9	0.094	0.010	10	
H8	0.073	0.011	10	
Hϵ	(0.089)		1	Only one spectrum available.
He I λ4026	0.076	0.008	9	
Si IV λ4089	0.024	0.005	4	Measured on low resolution spectra.
Si IV λ4116	w			Marginally detected on low resolution spectra.
He II λ4200	0.048	0.011	3	Blended with WR N III emissions.
He I λ4388	w			Blended with WR N III emissions.
He I λ4471	0.057	0.012	11	
He II λ4542	0.052	0.010	5	Blended with WR N III emissions.
C III λ4647	w			Only one spectrum available.
He II λ4686	($\leqq$0.081)		1	Very uncertain, only one spectrum available.
He I λ4713	w			Only one spectrum available.

w = line absent or too weak to be measured.

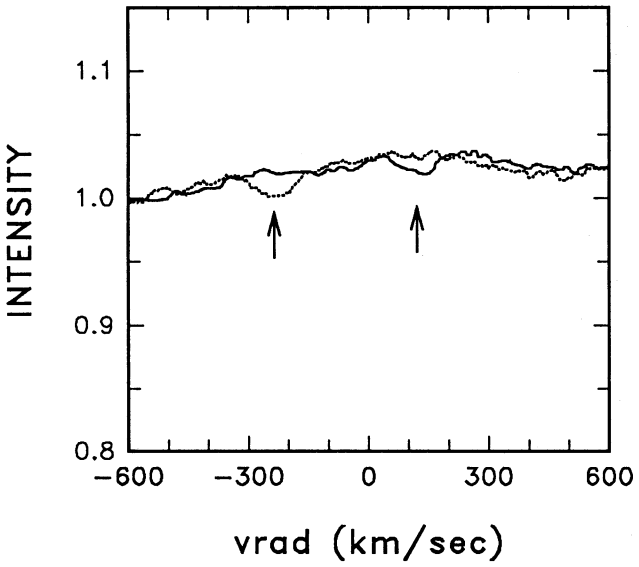

Fig. 3. High resolution CAT+CES spectra of WR 22 illustrating the detection of the companion for the He I λ4471 line. Radial velocities are relative to the WR star. The solid line corresponds to the spectrum taken at ϕ = 0.679, whereas the dotted line corresponds to ϕ = 0.103

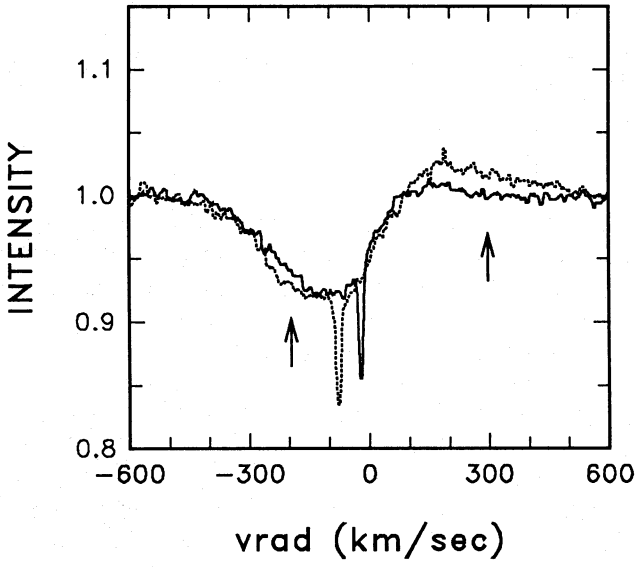

Fig. 4. Same as Fig. 3, but for the H8 Balmer line and phases ϕ = 0.688 (solid line) and ϕ = 0.034 (dotted line). One notices the narrow interstellar He I λ3889 absorption feature at a heliocentric radial velocity of –25 km s^{-1}

Some of the faintest lines were only detected once the radial velocity curve of the secondary was known. The detection of the companion is illustrated in Figs. 3, 4, 5 where pairs of observations taken at very different phases are presented. The individual CES spectra shown in these figures have been normalized and corrected for the orbital motion of the primary, so that the radial velocities are relative to the WR star. The positions of the secondary's absorptions are indicated by arrows.

Figure 3 illustrates the detection of the secondary in the case of the He I λ4471 line. The secondary's absorption is clearly visible around $v = -225$ km s^{-1} at ϕ = 0.103; it also appears around $v = +140$ km s^{-1} at ϕ = 0.679.

In a similar way, Fig. 4 displays the H8 Balmer line at phases ϕ = 0.034 and 0.688. While the red emission of the WR line is strongly absorbed at ϕ = 0.688, the auxiliary absorption appearing at ϕ = 0.034 seems to be much weaker. However, since this spectrum is taken immediately after periastron, it might well be affected by the eclipse of the O star by the WR wind or by some other effect due to binary interactions occurring at periastron.

Finally, Fig. 5 displays the spectral region around He II λ4200. The detection of the secondary's line is in good agree-

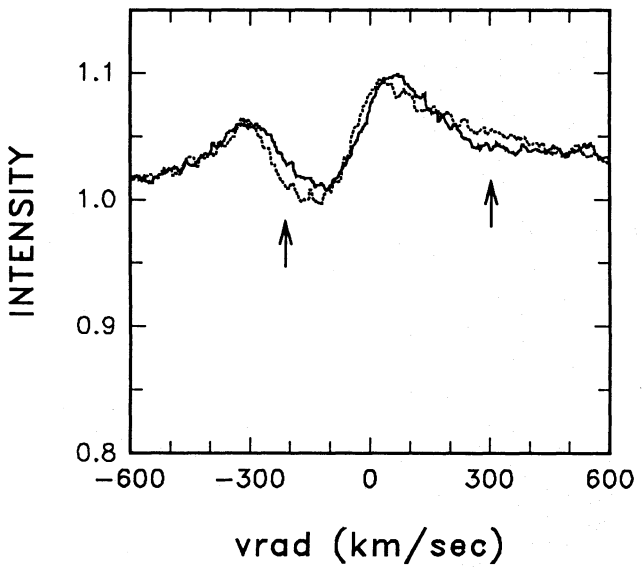

Fig. 5. Same as Fig. 3, but for the He II λ4200 line and phases $\phi = 0.928$ (solid line) and $\phi = 0.093$ (dotted line)

ment with the position predicted from the orbital solution described in Sect. 4.1.

4.1. Radial velocity curve

Only the most reliable RV's, i.e. those of He I λλ4026, 4471 and H9, were used to build up the radial velocity curve of the companion (Table 1). Given the larger uncertainties on the RV's of the companion (by comparison to those of the WR), the only free parameters used were γ and K, while the other parameters were given their value derived for the WR star. The resulting elements of the orbit are given in the last column of Table 3. One notices that the systemic velocity of the secondary is somewhat higher than the velocity of a sample of O stars belonging to the Carina OB1 association (which was found to lie between +5 and −25 km s^{-1}, CNW 1979), but this discrepancy might be due to the large uncertainties on the RV's of the secondary (the quoted uncertainties in Table 3 are probable errors, which means that the actual error could be larger). On the other hand, the γ velocity of the O star is quite different from the value we obtained for the N IV line of the WN7 primary. However, such differences are often encountered in WR + O binaries (e.g. Niemela & Moffat 1982, Niemela et al. 1980). The radial velocity curve of the secondary is shown in Fig. 6 along with the primary's solution for the N IV λ4058 emission and the H9 absorption (see Sect. 3). Part of the scatter of the H9 RV's in Fig. 2 can be explained from this figure. Indeed, immediately after periastron, the H9 line of the secondary moves towards negative velocities reaching the center of the WR absorption around $\phi = 0.03$. Between $\phi = 0.03$ and $\phi = 0.3$, the secondary's line creates an auxiliary absorption in the blue wing of the WR line, shifting the center of the resulting profile towards lower velocities. Between $\phi = 0.3$ and 0.7, it moves through the red wing of the WR absorption, leading to a slightly redshifted RV for the resulting blend. Beyond $\phi \sim 0.7$, the O star absorption crosses the emission wing of the profile and the RV of the absorption is no longer affected.

Using the results of Table 3, it is now possible to derive the physical characteristics of the components of the system. From the usual relations

$$\frac{m_{\rm WR}}{m_{\rm O}} = \frac{K_{\rm O}}{K_{\rm WR}} \tag{1}$$

and the mass function defined by

$$f(m_{\rm WR}) = \frac{m_{\rm O} \sin^3 i}{\left(\frac{m_{\rm WR}}{m_{\rm O}} + 1\right)^2} = \frac{1}{2\pi G} K_{\rm WR}^3 P (1 - e^2)^{\frac{3}{2}}, \tag{2}$$

one can evaluate the minimum masses of both stars. With $f(m_{\rm WR}) = 1.795\,{\rm M}_\odot$ and a mass ratio $\frac{m_{\rm WR}}{m_{\rm O}} = 2.78 \pm 0.14$, we find from Eq.(2) that $m_{\rm WR} \sin^3 i = 71.7 \pm 2.4\,{\rm M}_\odot$ and $m_{\rm O} \sin^3 i = 25.7 \pm 0.8\,{\rm M}_\odot$. Therefore, the WR star appears to be the most massive component of the binary. The minimum mass of the WN7+abs component of WR 22 derived here is significantly higher than the previous estimates. Smith & Maeder (1989) used the minimum mass $m_{\rm WR} \sin^3 i \gtrsim 40\,{\rm M}_\odot$ from CNW and the estimate of $i \lesssim 70°$ from M&S, to derive a value of $m_{\rm WR} \gtrsim 48\,{\rm M}_\odot$. The constraint on the inclination quoted by M&S was obtained from the absence of any eclipse in their photometric data obtained around $\phi = 0.5$ (O star in front of the WN7). However, WR 22 is known to display eclipses around $\phi = 0.0$ (WR in front of the O star, Balona et al. 1989, Gosset et al. 1991). Therefore, the absence of any noticeable occultation around apoastron must be interpreted as a result of the combination between inclination and eccentricity effects, and a reliable constraint on the inclination can only be obtained from a tailored model of the light curve of the eclipse. Crowther et al. (1995b) used the approximate mass-luminosity relation for O supergiants from Howarth & Prinja (1989) and the radiation-driven wind theory of Kudritzki et al. (1989) to estimate the current mass of the WN7+abs component to lie in the range of $29 - 53\,{\rm M}_\odot$. Finally, Hamann et al. (1995) use the mass-luminosity relation for pure helium stars given by Langer (1989) to compute the masses of their extensive sample of galactic WN stars. In the case of the WN7+abs component in WR 22, they derive a mass of $28.9\,{\rm M}_\odot$, which is indeed well below the minimum mass obtained in the present study. However, they notice that their estimate may not be adequate for those stars containing hydrogen, as does WR 22.

4.2. Spectral classification

In order to assign a spectral subtype and luminosity class to the secondary, one has to measure the equivalent widths of its lines. This turns out to be quite difficult, since the relevant lines are weak and are often blended with the WR lines. Therefore, a first step is to correct each spectrum for the orbital motion of the WN7, before dividing it by an unblended reference profile of the WR line. This reference profile is constructed using several spectra taken at quite different phases. Since the division by the unblended profile is one of the most critical steps,

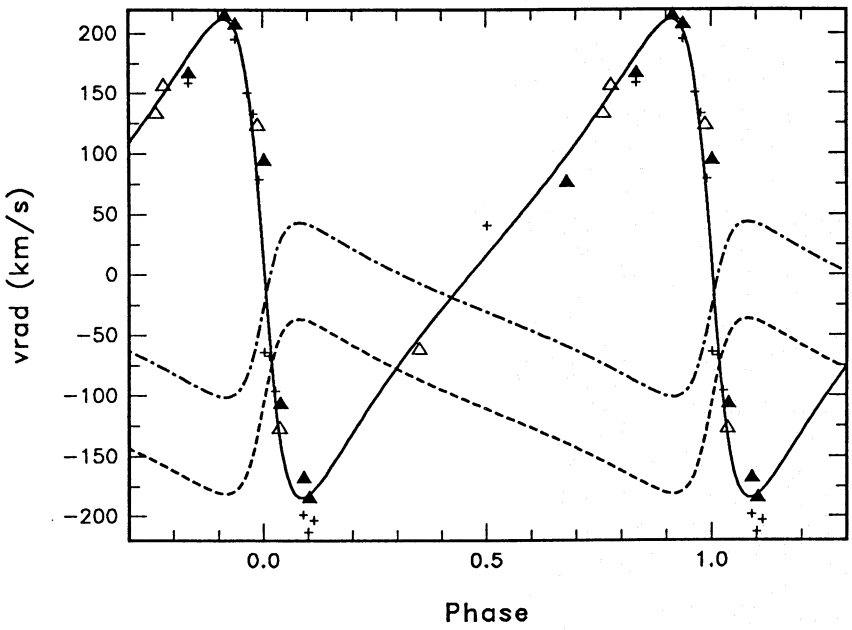

Fig. 6. Radial velocities of the WR 22 secondary's lines. Crosses indicate He I λ4026 observations while open and filled triangles indicate H9 and He I λ4471 respectively. The solid line shows the resulting orbital solution for the companion, while the dashed-dotted and the dashed lines show the orbital solution of the WR star derived from the N IV λ4058 emission and the H9 absorption respectively

at least two different measurements were carried out for each spectrum, adopting either an optimistic or a pessimistic estimate of the reference profile. Then, equivalent widths measured on the resulting "reduced" spectra have to be multiplied by a correction coefficient $\overline{P}$, i.e. the observed line-to-continuum ratio (Cherepashchuk et al. 1995), in order to obtain the equivalent widths W_λ of the O star lines in the WR + O binary. The values listed in Table 4 are the resulting means on all the spectra where the line is detected unambiguously and is not affected by any eclipsing effect from the WR wind. The uncertainties quoted in Table 4, estimated from the standard deviations of the individual values, are rather large, due to the weakness of the lines.

According to Conti's (1973b) classification, the value of

$$\log_{10} W'_\lambda = \log_{10}\left(\frac{W_\lambda(4471)}{W_\lambda(4542)}\right) \quad (3)$$

i.e. the line ratio $\lambda\lambda$4471 He I/4542 He II, unambiguously determines the spectral type of an O star. Since one is dealing here with lines in a rather narrow spectral domain, no correction is needed for the slope of the continuum (see however Sect. 4.3 below). In our case we have $W_\lambda(4471) = 0.0573 \pm 0.0116$ Å and $W_\lambda(4542) = 0.0520 \pm 0.0103$ Å leading to $-0.135 \leqq \log_{10} W'_\lambda \leqq 0.218$ with a mean value of 0.042. Using the quantitative criterion of Conti (Conti & Alschuler 1971, Mathys 1988), we obtain a late O-type star (O6.5–O8.5 with a mean type of O7.5).

Several luminosity criteria have been suggested for O stars. Conti & Alschuler (1971) used the ratio of the equivalent widths of the lines Si IV λ4089 and He I λ4143, whereas Mathys (1988) defines luminosity classes according to the nature and strength of the He II λ4686 line. Neither of these criteria can be used in our case since all the relevant lines are either not detected or too weak to be measured with a sufficient accuracy.

4.3. Luminosity ratio

An upper limit on the continuum-luminosity ratio at 5500 Å i.e. $q = L^y_{\rm WR}/L^y_{\rm O}$ can be set from the depth of the eclipses. From Gosset et al. (1991), it follows that the occultation of the O star by the WR leads to a variation of magnitude in the Strömgren y filter of $\Delta y \sim 0.083$ mag. In the case of a total eclipse of the secondary by the WN7+abs star, one gets

$$\Delta y = -2.5 \log_{10}\left(\frac{q_{\rm up}}{1+q_{\rm up}}\right) \quad (4)$$

leading to $q \lesssim q_{\rm up}$ with $q_{\rm up} \cong 12.6$.

An independent way to estimate q from spectroscopic data is described by Cherepashchuk et al. (1995). The absorption lines of the O star in the combined spectrum of WR 22 are diluted by the radiation of the WN7 component. Therefore, it follows from Cherepashchuk et al. (1995) that

$$q_\lambda = \frac{W_\lambda^{\rm sing}}{W_\lambda} - 1 \quad (5)$$

where W_λ is the equivalent width of the O star line measured on the combined spectrum of the binary and $W_\lambda^{\rm sing}$ is the equivalent width of the same line as seen in single O star spectra. In order to compare q_λ obtained from Eq.(5) to q at 5500 Å, one has to take into account the different slopes of the continua of the WR and of the O star. This can be done by evaluating the ratio

$$k = \frac{F^{WR}_{5500}}{F^{WR}_\lambda}\frac{F^O_\lambda}{F^O_{5500}}. \quad (6)$$

The first term of the right-hand side expression was estimated using a power law $F_\lambda \sim \lambda^{-\alpha}$ with $<\alpha>_{WNL} = 2.87 \pm 0.38$ (Morris et al. 1993), while the second term was evaluated from the models of Kurucz (1979) and from a direct measurement on spectra taken from the library of Jacoby et al. (1984).

Table 5. Luminosity ratio q derived from spectroscopic data. The quoted errors are 1σ standard deviations taking into account the errors on our measured W_λ's and the scatter within a given spectral type in the data of Conti & Alschuler (1971) and Conti (1973a)

Line	O6.5		O7		O7.5		O8		O8.5	
	$W_\lambda^{\rm sing}$	q	$W_\lambda^{\rm sing}$	q	$W_\lambda^{\rm sing}$	q	$W_\lambda^{\rm sing}$	q	$W_\lambda^{\rm sing}$	q
He I λ4026	0.62	5.7 ± 1.5	0.61	5.5 ± 1.7	0.65	6.0 ± 1.5	0.74	6.9 ± 1.8	0.77	7.2 ± 1.6
He I λ4471	0.54	7.3 ± 2.1	0.59	7.9 ± 3.0	0.71	9.7 ± 3.0	0.85	11.9 ± 3.4	0.86	11.9 ± 3.5
He II λ4200	0.49	7.4 ± 2.6	0.59	9.1 ± 3.1	0.42	6.2 ± 2.5	0.45	6.8 ± 2.7	0.40	5.9 ± 2.5
He II λ4542	0.78	11.8 ± 3.6	0.67	10.1 ± 3.9	0.64	9.6 ± 3.0	0.60	9.0 ± 2.4	0.49	7.2 ± 2.1

Equivalent widths of He I $\lambda\lambda$4026, 4471, He II $\lambda\lambda$4200 and 4542 were taken from Conti & Alschuler (1971) and Conti (1973a). The sensitivity of these lines to the luminosity class is rather low. For each relevant spectral type, mean equivalent widths over all luminosity classes were evaluated and used as comparison values $W_\lambda^{\rm sing}$ in Eq.(5). The resulting luminosity ratios at 5500 Å are listed in Table 5. The uncertainties are estimated taking into account the errors on our measured W_λ as well as the dispersion of $W_\lambda^{\rm sing}$ within a given spectral type. One notices from Table 5 that nearly all the individual values of q are in agreement with the upper limit of 12.6 derived from the photometric data. The mean $\overline{q} = 8.2$ indicates that the WN7+abs star should be about 2.3 magnitudes brighter than its O7.5 companion.

There are less data available in the literature for the lines of the upper Balmer series in single O stars. Moreover, the equivalent widths of these lines show a significant sensitivity to the luminosity class. The most extensive data were found in Oke (1954) who studied equivalent widths for 5 stars of spectral types O7-O8 and luminosity classes I–III. Additional measurements were made on the 14 late O star spectra of the Jacoby et al. (1984) library. The corresponding results are listed in Table 6.

The q values derived from H9 and H10 are in reasonable agreement with the results from the helium lines. Although the H8 line sometimes leads to a q value somewhat higher than $q_{\rm up}$, this discrepancy may not be significant and could simply reflect the uncertainties on our W_λ-values (due especially to the blend with the interstellar He I λ3889 line around several phases).

From the above analysis of the Balmer series, a giant or supergiant luminosity class appears to give the best agreement between the luminosity ratio derived from the hydrogen lines and from the helium lines. However, since WR 22 is a member of the Carina OB1 association, its absolute magnitude is rather well known. Assuming a colour excess of $E_{b-v} = 0.33$ mag (Schmutz et al. 1989), one gets an absolute magnitude $M_v^{\rm WR} = -7.0$ mag (Hamann et al. 1991) and a continuum luminosity ratio of the order of 8 leads to an absolute magnitude of the secondary of $M_v^{\rm O} = -4.7$ mag. According to the M_v-spectral type relation for O stars (Conti et al. 1983, Howarth & Prinja 1989), this would correspond to a main sequence secondary. Therefore, further evidence is needed to ascertain the luminosity class of the secondary.

5. Discussion and conclusion

Among the double-lined (SB2) WR + O binaries studied by Massey (1981), only one system (the contact binary CQ Cep) is classified as WN7 + O. It is worth noticing that this is the only binary in Massey's sample with a mass ratio $m_{\rm WR}/m_{\rm O}$ above unity (~ 1.19), while the mean mass ratio lies between 0.3 and 0.5. However, the actual value of the CQ Cep mass ratio is still a matter of debate (see e.g. Antokhina & Cherepashchuk 1988) and recently Marchenko et al. (1995) classified CQ Cep as a WN6 + O system with a mass ratio below unity. With a mass ratio of 2.78, WR 22 appears therefore to be very unusual. In fact, most of the modern evolutionary scenarios of massive O + O binaries, especially those including mass transfer by Roche lobe overflow (RLOF), predict mass ratios of the resulting WR + O system well below unity (De Greve et al. 1988, Schulte-Ladbeck 1989). However, Maeder & Meynet (1994) argued that stellar winds become much more important than RLOF mass transfer in the inner metal-rich galactic regions and therefore very massive primaries in O + O systems may evolve into the WR stage through mass loss by stellar wind only. Consequently, WR 22 could result from a very massive progenitor evolving nearly independently of its companion. Further evidence for this suggestion comes from the large eccentricity of the orbit, although De Greve (1991) argued that circularisation times are always much longer than main sequence lifetimes and there fore long period, eccentric systems could well be formed through mass transfer without circularisation of the orbit.

The exceptionally high mass of the WN7 star ($m_{\rm WR} \geqq 72 M_\odot$, while the mean WR mass lies around 20 $M_\odot$, Massey 1981) and the high hydrogen mass-fraction (Hamann et al. 1991, Crowther et al. 1995a) suggest that WR 22 is at the beginning of its WR evolution. According to Langer et al. (1994), the evolution of massive stars proceeds through the sequence O → Of → H-rich WN → LBV → H-poor WN → H-free WN → WC → SN. In this scenario, luminous H-rich late type WN stars are identified as core hydrogen burning objects. The discrepancy between the minimum mass derived here and the prediction from the mass-luminosity relation given by Langer (1989) for pure helium stars may well indicate that the WN7+abs star in WR 22 could be such a core hydrogen burning star. Crowther et al. (1995b) prefer a different scenario for the most massive stars ($m_{\rm initial} \geqq 60 M_\odot$) in which they give a specific role to the WNL+abs subclass: O → Of → WNL+abs → WN7 (→ WNE) → WC → SN. Although our present results do not al-

Table 6. Luminosity ratio from the hydrogen lines. W_λ^{sing} are taken from: (1) Jacoby et al. (1984) and (2) Oke (1954). For each luminosity class the range of W_λ^{sing} values is given

	H8		H9		H10	
	W_λ^{sing}	q	W_λ^{sing}	q	W_λ^{sing}	q
O6.5-O9 V (1)	1.55-2.21	20.2-29.3	1.09-1.84	10.6-18.6		
O6.5-O8.5 III (1)	1.14-1.89	11.2-19.2	1.05-1.75	7.6-13.2		
O7-O8 III (2)	1.13-1.97	11.2-20.1	1.09-1.54	8.0-11.5	0.80-1.44	6.6-12.5
O7-O8 I (2)	1.09-1.33	10.8-13.3	0.80-1.20	5.6-8.8	0.85-1.00	7.1-8.5

low a clear choice between these two scenarios, they indicate that, indeed, the WN7+abs star in WR 22 had a very massive progenitor which evolved mainly through mass loss by stellar wind (by opposition to Roche lobe overflow).

In conclusion, we have probably identified a representative of a rather poorly populated class of WR stars, even if its existence has been predicted many years ago (Conti, 1976). Indeed, while most of the WR are highly evolved helium burning descendants of massive O stars, here, we are most probably dealing with a core hydrogen burning object. This means that, while its core is still the one of a main sequence object, the external layers of WR 22 have been nearly completely peeled off, leading to reduced H and enhanced He and N abundances at the surface. At the same time, the star has developed a higher density wind than typical Of stars, giving it the external appearance of a WR object.

Acknowledgements. The authors express their thanks to W.-R. Hamann for performing model calculations at their request and to J.-F. Claeskens for taking the 1994 spectra of WR 22; their thanks also go to V.S. Niemela and P. Morris for discussions and to J.-P. Swings who significantly improved a first version of the manuscript. Enlightening comments by P.S. Conti are also appreciated. The authors are greatly indebted to the Fonds National de la Recherche Scientifique (Belgium) for multiple supports. This research is also supported in part by contracts ARC 90/94-140 and ARC 94/99-178 "Action de recherche concertée de la Communauté Française" (Belgium) and by contract SC005 of the belgian programme "Service Centers and Research Networks" initiated by the Belgian State, Prime Minister's Office, Science Policy Programming under SSTC. Partial support through the PRODEX XMM-OM Project is also gratefully acknowledged. The SIMBAD database has been consulted for the bibliography.

References

Antokhina, E.A., Cherepashchuk, A.M. 1988, SvA, 32, 531
Balona, L.A., Egan, J., Marang, F. 1989, MNRAS, 240, 103
Cherepashchuk, A.M., Koenigsberger, G., Marchenko, S.V., Moffat, A.F.J. 1995, A&A, 293, 142
Conti, P.S. 1973a, ApJ, 179, 161
Conti, P.S. 1973b, ApJ, 179, 181
Conti, P.S. 1976, Mém. Soc. Roy. Sci. Liège Série 6, 9, 193
Conti, P.S., Alschuler, W.R. 1971, ApJ, 170, 325
Conti, P.S., Garmany, C.D., de Loore, C., Vanbeveren, D. 1983, ApJ, 274, 302
Conti, P.S., Niemela, V.S., Walborn, N.R. 1979, ApJ, 228, 206
Crowther, P.A., Hillier, D.J., Smith, L.J. 1995a, A&A, 293, 403
Crowther, P.A., Smith, L.J., Hillier, D.J., Schmutz, W. 1995b, A&A, 293, 427
De Greve, J.P. 1991, in *Wolf-Rayet Stars and Interrelations with Other Massive Stars in Galaxies*, IAU Symp. No. 143, eds. K.A. van der Hucht and B. Hidayat, Kluwer, Dordrecht, p.213
De Greve, J.P., Hellings, P., van den Heuvel, E.P.J. 1988, A&A, 189, 74
Dennefeld, M., Guttin Lombard, B., Le Luyer, M., Rossignol, P. 1979, ESO Technical Note, IDG 120-79
Gosset, E., Magain, P. 1993, The Messenger, 73, 13
Gosset, E., Remy, M., Manfroid, J., Vreux, J.-M., Balona, L.A., Sterken, C., Franco, G.A.P. 1991, *Inf. Bull. Var. Stars*, 3571
Hamann, W.-R. 1995, private communication
Hamann, W.-R., Dünnebeil, G., Koesterke, L., Schmutz, W., Wessolowski, U. 1991, A&A, 249, 443
Hamann, W.-R., Koesterke, L., Wessolowski, U. 1995, A&A, in press
Howarth, I.D., Prinja, R.K. 1989, ApJS, 69, 527
Jacoby, G.H., Hunter, D.A., Christian, C.A. 1984, ApJS, 56, 257
Kudritzki, R.P., Pauldrach, A.W.A., Puls, J., Abbott, D.C. 1989, A&A, 219, 205
Kurucz, R.L. 1979, ApJS, 40, 1
Lafler, J., Kinman, T.D. 1965, ApJS, 11, 216
Langer, N. 1989, A&A, 210, 93
Langer, N., Hamann, W.-R., Lennon, M., Najarro, F., Pauldrach, A.W.A., Puls, J. 1994, A&A, 290, 819
Lundström, I., Stenholm, B. 1984, A&AS, 58, 163
Maeder, A., Conti, P.S. 1994, Ann. Rev. Astron. Astrophys., 32, 227
Maeder, A., Meynet, G. 1994, A&A, 287, 803
Marchenko, S.V., Moffat, A.F.J., Eenens, P.R.J., Hill, G.M., Grandchamps, A. 1995 ApJ in press
Massey, P. 1981, ApJ, 246, 153
Mathys, G. 1988, A&AS, 76, 427
Meynet, G., Maeder, A., Schaller, G., Schaerer, D., Charbonnel, C. 1994, A&AS, 103, 97
Moffat, A.F.J., Seggewiss, W. 1978, A&A, 70, 69
Morris, P.W., Brownsberger, K.R., Conti, P.S., Massey, P., Vacca, W.D. 1993, ApJ, 412, 324
Niemela, V.S. 1973, PASP, 85, 220
Niemela, V.S. 1979, in *Mass Loss and Evolution of O-Type Stars*, IAU Symp. No. 83, eds. P.S. Conti and C.W.H. de Loore, Reidel, Dordrecht, p.291
Niemela, V.S., Conti, P.S., Massey, P. 1980, ApJ, 241, 1050
Niemela, V.S., Moffat, A.F.J. 1982, ApJ, 259, 213
Oke, J.B. 1954, ApJ, 120, 22
Rauw, G., Vreux, J.-M., Gosset, E., Hutsemékers, D., Magain, P., Manfroid, J., Remy, M., Rochowicz, K. 1995, in *Wolf-Rayet Stars: Bi-*

naries, Colliding Winds, Evolution, IAU Symp. No. 163, eds. K.A. van der Hucht and P.M. Williams, Kluwer, Dordrecht, p.241
Schmutz, W., Hamann, W.-R., Wessolowski, U. 1989, A&A, 210, 236
Schulte-Ladbeck, R. 1989, AJ, 97, 1471
Schwarz, H.E., Melnick, J. 1993, *The ESO Users Manual 1993*
Smith, L.F., Maeder, A. 1989, A&A, 211, 71
van der Hucht, K.A., Conti, P.S., Lundström, I., Stenholm, B. 1981, Space Sci. Rev., 28, 227
van der Hucht, K.A., Hidayat, B., Admiranto, A.G., Supelli, K.R., Doom, C. 1988, A&A, 199, 217
Vreux, J.-M., Dennefeld, M., Andrillat, Y. 1983, A&AS, 54, 437
Walborn, N.R., Hesser, J.E. 1975, ApJ, 199, 535
Wolfe, R.H.Jr., Horak, H.G., Storer, N.W. 1967, in *Modern Astrophysics*, ed. M. Hack, Gordon & Breach, New York, p.251

This article was processed by the author using Springer-Verlag LaTeX A&A style file version 3.